

# Earthquake source parameters for the 2010 western Gulf of Aden rifting episode

Ashley Shuler<sup>1,2</sup> and Meredith Nettles<sup>1,2</sup>

<sup>1</sup>Lamont-Doherty Earth Observatory of Columbia University, New York, NY, USA. Email: ashuler@ldeo.columbia.edu

<sup>2</sup>Department of Earth and Environmental Sciences, Columbia University, New York, NY, USA

Accepted 2012 April 26. Received 2012 April 26; in original form 2011 October 17

## SUMMARY

On 2010 November 14, an intense swarm of earthquakes began in the western Gulf of Aden. Within a 48-hr period, 82 earthquakes with magnitudes between 4.5 and 5.5 were reported along an ~80-km-long segment of the east–west trending Aden Ridge, making this swarm one of the largest ever observed in an extensional oceanic setting. In this study, we calculate centroid-moment-tensor solutions for 110 earthquakes that occurred between 2010 November and 2011 April. Over 80 per cent of the cumulative seismic moment results from earthquakes that occurred within 1 week of the onset of the swarm. We find that this sequence has a *b*-value of ~1.6 and is dominated by normal-faulting earthquakes that, early in the swarm, migrate westwards with time. These earthquakes are located in rhombic basins along a section of the ridge that was previously characterized by low levels of seismicity and a lack of recent volcanism on the seafloor. Body-wave modelling demonstrates that the events occur in the top 2–3 km of the crust. Nodal planes of the normal-faulting earthquakes are consistent with previously mapped faults in the axial valley. A small number of strike-slip earthquakes observed between two basins near 44°E, where the axial valley changes orientation, depth and width, likely indicate the presence of an incipient transform fault and the early stages of ridge-transform segmentation. The direction of extension accommodated by the earthquakes is intermediate between the rift orthogonal and the direction of relative motion between the Arabian and Somalian plates, consistent with the oblique style of rifting occurring along the slow-spreading Aden Ridge. The 2010 swarm shares many characteristics with dyke-induced rifting episodes from both oceanic and continental settings. We conclude that the 2010 swarm represents the seismic component of an undersea magmatic rifting episode along the nascent Aden Ridge, and attribute the large size of the earthquakes to the combined effects of the slow spreading rate, relatively thick crust and recent quiescence. We estimate that the rifting episode was caused by dyke intrusions that propagated laterally for 12–18 hr, accommodating ~1–14 m of opening or ~85–800 yr of spreading along this section of the ridge. Our findings demonstrate the westward propagation of active seafloor spreading into this section of the western Gulf of Aden and illustrate that deformation at the onset of seafloor spreading may be accommodated by discrete episodes of faulting and magmatism. A comparison with similar sequences on land suggests that the 2010 episode may be only the first of several dyke-induced rifting episodes to occur in the western Gulf of Aden.

**Key words:** Earthquake source observations; Seismicity and tectonics; Body waves; Mid-ocean ridge processes; Submarine tectonics and volcanism; Africa.

## 1 INTRODUCTION

The Gulf of Aden is a young ocean basin that stretches from the Afar depression in East Africa to the Carlsberg Ridge in the Indian Ocean (Fig. 1). Here, northeastward motion of the Arabian plate relative to the Somalian plate is accommodated by oblique spreading on a system of approximately east–west trending rift zones (Courtillot

1980; Cochran *et al.* 1981; Manighetti *et al.* 1997; Bosworth *et al.* 2005). Beginning in mid-November 2010, the western Gulf of Aden between 43.75° and 44.5°E experienced an intense swarm of earthquakes. Within a 48-hr period, 24 earthquakes with magnitudes between 5.0 and 5.5, and 58 earthquakes with magnitudes between 4.5 and 5.0, were reported in this area. The magnitudes of these earthquakes, as well as the large number of earthquakes in a short time,

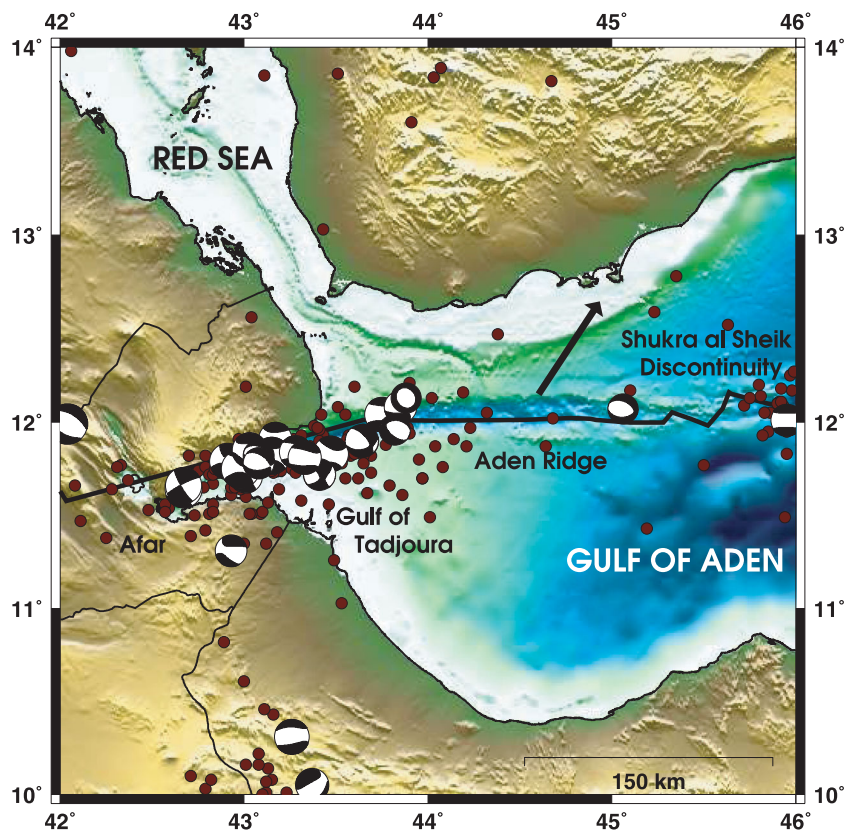


**Figure 1.** Map of the western Gulf of Aden and surroundings. The Carlsberg Ridge lies east of the Shukra al Sheik discontinuity, outside the frame of the figure. Maroon dots mark the locations of earthquakes in the NEIC catalogue (1973–2010). Focal mechanisms are from the Global CMT catalogue (1976–2010). All seismic data plotted covers the entire period of the catalogues before the start of the earthquake swarm. Plate boundary information is from Bird (2003). The plate motion vector for the Arabian plate relative to the Somalian plate ( $1.6 \text{ cm yr}^{-1}$  at  $\text{N}34^\circ\text{E}$ ) is from MORVEL (DeMets *et al.* 2010). Topography and bathymetry is plotted from the GEBCO\_08 Grid, version 20100927, <http://www.gebco.net>.

make this swarm one of the largest ever observed in an extensional oceanic setting. Teleseismically detected earthquakes continued to occur for several months after the onset of the swarm, although at a much lower rate. The earthquake sequence occurred on a tectonically complex section of the Aden Ridge, crossing structural and mechanical boundaries (Dauteuil *et al.* 2001; Hébert *et al.* 2001). In this paper, we use data from the Global Seismographic Network (GSN) to estimate source parameters for 110 earthquakes in the sequence, allowing us to characterize the swarm and better constrain the tectonics of this nascent spreading centre. Comparison with seismic and volcanic activity in other regions suggests the swarm represents the seismic component of an undersea rifting episode, the first documented in this area.

## 2 TECTONIC BACKGROUND

The impingement of the Afar mantle plume on the base of the African lithosphere  $\sim 31$  Ma triggered continental rifting in the Gulf of Aden (Baker *et al.* 1996; Hoffman *et al.* 1997; Rochette *et al.* 1997; Ukstins *et al.* 2002; Bosworth *et al.* 2005). This event, combined with regional extension resulting from the subduction of Africa beneath Eurasia (Malkin & Shemenda 1991; Courtillot *et al.* 1999; Jolivet & Faccenna 2000; Bellahsen *et al.* 2003; Bosworth *et al.* 2005) resulted in the initiation of seafloor spreading in the eastern Gulf of Aden. Extension propagated westwards over time, reaching the Shukra al Sheik discontinuity, and the eastern edge of

the Afar plume, approximately 10 Ma (Bosworth *et al.* 2005). Rifting stalled there, and propagated into the central and western Gulf of Aden only within the last 2–3 Ma (Cochran 1981; Bosworth *et al.* 2005). Gravity and magnetic data have indicated that the western boundary of active seafloor spreading is currently at approximately  $44^\circ\text{E}$  (Hébert *et al.* 2001). East of the Shukra al Sheik discontinuity, the crust is oceanic with a mean thickness of 6 km, and extension is accommodated by faulting and oceanic accretion along a well-developed ridge-transform system (Dauteuil *et al.* 2001). In the area of the 2010 earthquake swarm, however, the crustal thickness ranges from 6 to 13 km, and although an axial trough is present, ridge-transform segmentation is poorly developed (Dauteuil *et al.* 2001). This section of the Aden Ridge is part of a  $\sim 130$ -km-long transition between oceanic lithosphere in the east and stretched continental lithosphere in the west (Dauteuil *et al.* 2001; Hébert *et al.* 2001).

The Aden Ridge spreads at a rate of  $1.6 \text{ cm yr}^{-1}$  in the direction  $\text{N}34^\circ\text{E}$  (DeMets *et al.* 2010; Fig. 1). The spreading direction is oblique to the rift axis, which trends  $\text{N}90^\circ\text{E}$  between the Shukra al Sheik discontinuity and  $\sim 44^\circ\text{E}$  longitude, and  $\text{N}70^\circ\text{E}$  as it approaches the Gulf of Tadjoura. East of  $44^\circ\text{E}$ , the axial valley is between 1000 and 1500 m deep and has a mean width of 20 km. Acoustic reflectivity surveys have shown that this portion of the ridge consists of overlapping rhombic basins oriented  $\text{N}120^\circ\text{E}$  (Manighetti *et al.* 1997; Dauteuil *et al.* 2001). The axial valley is bounded by east–west trending normal faults whereas the centre of the valley contains left-stepping en echelon faults oriented  $\text{N}100$ – $120^\circ\text{E}$  that

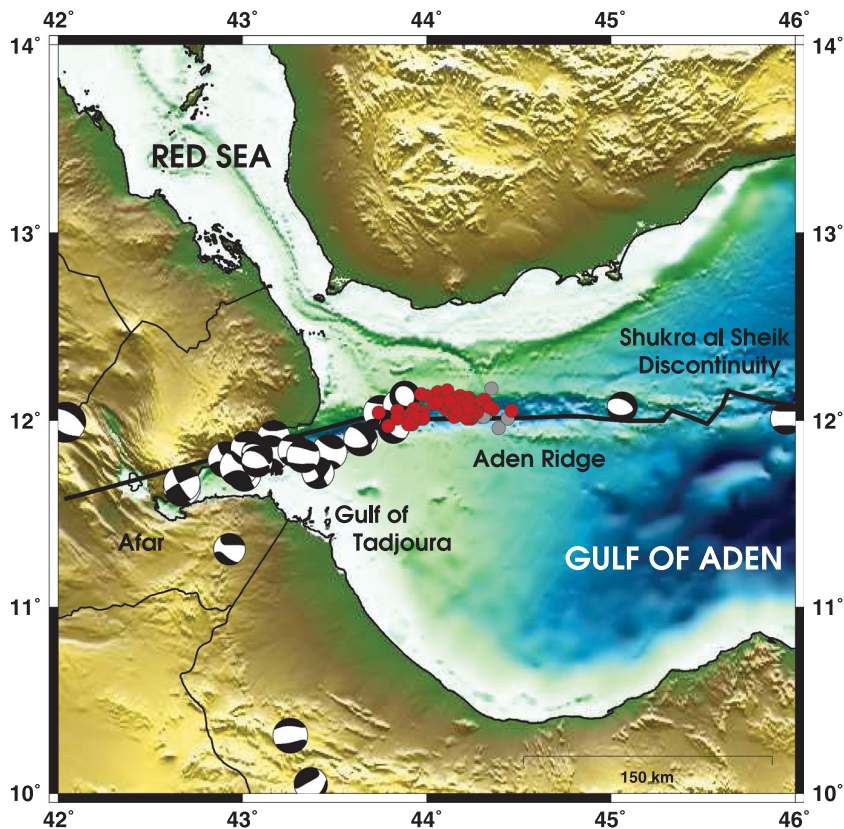


**Figure 2.** Centroid locations for 110 earthquakes analysed in this study (2010 November–2011 April). Red dots denote earthquakes with well-constrained locations and grey dots denote earthquakes with less-well-constrained locations. Focal mechanisms, plate boundary information, bathymetry and topography are as in Fig. 1.

accommodate both extension and right-lateral strike-slip motion (Manighetti *et al.* 1997; Dauteuil *et al.* 2001). West of 44°E, the axial valley changes orientation, deepens to 1650 m and narrows to a width of 10–15 km. There the ridge is composed of several basins containing linear to sigmoidal normal faults striking N80°–N120°E (Tamsett & Searle 1988; Taylor *et al.* 1994; Tuckwell *et al.* 1996; Dauteuil *et al.* 2001). Backscatter images from a 1995 cruise showed no recent lava flows or volcanic cones between 43.3° and 44.3°E (Dauteuil *et al.* 2001).

### 3 SEISMIC OVERVIEW

The section of the Aden Ridge that ruptured during the 2010 swarm was previously characterized by low levels of seismicity (Fig. 1). Before 2010, the area between 43.9°E and 45°E had not ruptured in a  $M_5+$  earthquake in at least the last 38 yr, the era of modern seismic instrumentation and the time span covered by the catalogues of the USGS National Earthquake Information Center (NEIC; 1973–present) and Global Centroid Moment Tensor Project (GCMT; 1976–present; Dziewonski *et al.* 1981; Ekström *et al.* 2005). This contrasts with other sections of the ridge, including the Gulf of Tadjoura near the Afar triple junction and the Sheba Ridge east of the Shukra al Sheik discontinuity, where moderate-sized earthquakes occur frequently.

The 2010 western Gulf of Aden earthquake sequence was preceded by a  $M_w$  4.5 earthquake on November 13 at 18:26 GMT. The main part of the sequence began 12 hr later on November 14 at 06:32 with a  $M_w$  5.4 earthquake. Over the next 48 hr, 82 earthquakes with magnitudes 4.5 and greater were located by the NEIC

and/or by the GCMT Project using surface waves (Ekström 2006; Fig. 2). The number of moderate-sized earthquakes in this sequence is extraordinary, and is comparable to the number of similarly sized earthquakes expected in the aftershock sequence of a  $M_w$  7–8 main shock (Shcherbakov & Turcotte 2004; Shcherbakov *et al.* 2005), even though the largest earthquake was only  $M_w$  5.5. Seventy per cent of the cumulative seismic moment of the swarm results from earthquakes occurring the first day, and 83 per cent from earthquakes occurring the first week (Fig. 3). Earthquakes were detected in the area through 2011 August, although they occurred at a much lower rate than during the swarm.

### 4 DATA AND METHODS

We use data from the IRIS–USGS GSN, Geoscope, GEOFON, MEDNET and the Canadian Regional Seismic Network to calculate centroid moment tensors, locations and times for earthquakes in the western Gulf of Aden between 2010 November and 2011 April, the first 6 months after the start of the swarm. We calculate centroid-moment-tensor solutions generally following the standard GCMT approach for earthquakes with  $M_w < 5.5$  (Dziewonski *et al.* 1981; Arvidsson & Ekström 1998; Ekström *et al.* 2005), which incorporates long-period body waves filtered from 40–150 s and intermediate-period surface waves filtered from 50–150 s. Solutions for the smallest earthquakes are constrained primarily by surface-wave data, and in this case, we adjust the filter to shorter periods (40–100 or 35–75 s) on a case-by-case basis to increase the signal-to-noise ratio. Data from 30–100 stations are used for each solution,



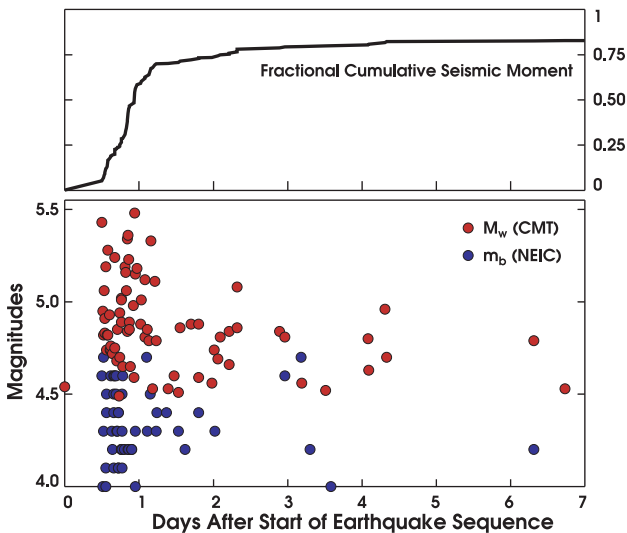


**Figure 3.** Top: Fractional cumulative seismic moment during the first week of the 2010 Gulf of Aden earthquake sequence. The cumulative seismic moment is estimated by summing the scalar moments for earthquakes analysed in this study. The cumulative seismic moment through 2011 April is  $3.5 \times 10^{18}$  Nm, which is equivalent to a single  $M_w$  6.3 earthquake. Bottom: Times and magnitudes of earthquakes. Red dots show moment magnitudes for earthquakes analysed in this study. Blue dots show times and magnitudes for additional earthquakes reported by the USGS NEIC; these are not included in the moment sum.

with the nearest station being FURI-IU, located  $\sim 675$  km away near Addis Ababa, Ethiopia.

Because all of the earthquakes in the western Gulf of Aden swarm are shallow, their depths cannot be resolved well with the long-period seismic data used in standard GCMT analysis. Likewise, depth estimates could not easily be read from depth phases because the direct and reflected teleseismic  $P$  waves for shallow normal-faulting earthquakes typically have opposite polarity and occur very close together in time. To obtain accurate estimates of focal depth, we model the broad-band teleseismic body waves of the largest earthquakes of the sequence ( $M_w \geq 5.2$ ) using the method of Ekström (1989). We perform an inversion of  $P$  and  $SH$  wave-

forms for focal mechanism, focal depth and moment-rate function. For this analysis, we deconvolve the instrument response to obtain broad-band displacement records filtered from 1–100 s period. Synthetic seismograms are calculated using ray theory and the Preliminary Reference Earth Model (Dziewonski & Anderson 1981). Reflections and conversions near the source are modelled using a layer-matrix method for a regional velocity model. We use the CRUST2.0 velocity model for the Red Sea (Y0—thinned continental crust with 1.0-km thick sediment layer; Bassin *et al.* 2000), adding a 1.25-km thick water layer on top to match local bathymetry. The CMT estimate of the point-source moment tensor is included as a soft constraint in the inversion to ensure that focal mechanisms calculated from the broad-band data are compatible with the long-period data used in CMT analysis.

## 5 RESULTS

We are able to obtain CMT solutions for 110 earthquakes of the western Gulf of Aden sequence and broad-band body-wave estimates of depth for four of the larger events. These results are summarized in Figs 4–7, and source parameters are provided in Tables 1, S1 and S2 (see the Supporting Information section), and in electronic format on our web site ([www.globalcmt.org](http://www.globalcmt.org)). Below, we examine the source parameters retrieved in the context of known geology, and, in Section 6, consider implications of the sequence in light of the tectonic setting and ongoing evolution of the Gulf of Aden.

### 5.1 Centroid-moment-tensor solutions

We attempted to analyse all 198 earthquakes with initial magnitudes of 4.0 or larger as reported by the NEIC and/or the GCMT Project, and were able to obtain CMT solutions for 110 earthquakes with magnitudes  $4.5 \leq M_w \leq 5.5$  (Fig. 3). Solutions for the 25 largest earthquakes, those with  $M_w \geq 5.0$ , have been adopted as the preferred solutions of the GCMT catalogue, which has a minimum magnitude threshold of  $M \sim 5$ . We consider both these and our additional 85 solutions for smaller events here. Focal mechanisms are presented in Fig. 4. The solutions are generally robust and well constrained. In the figures and tables, we identify 18 earthquakes as having less well-constrained focal mechanisms. This designation

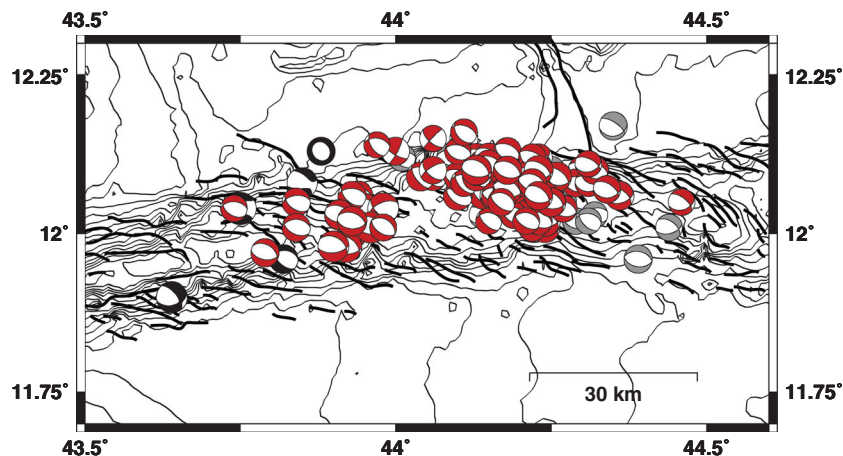


**Figure 4.** Focal mechanisms for the western Gulf of Aden. Black focal mechanisms are pre-swarm earthquakes from the Global CMT catalogue. Focal mechanisms for the sequence that began on 2010 November 13 are plotted in red and grey, with only the double-couple component shown. The best-constrained focal mechanisms are plotted in red, and the less well-constrained focal mechanisms are plotted in grey. Black lines show fault traces from Dauteuil *et al.* (2001). Bathymetry from GEBCO is plotted in 100-m contours.

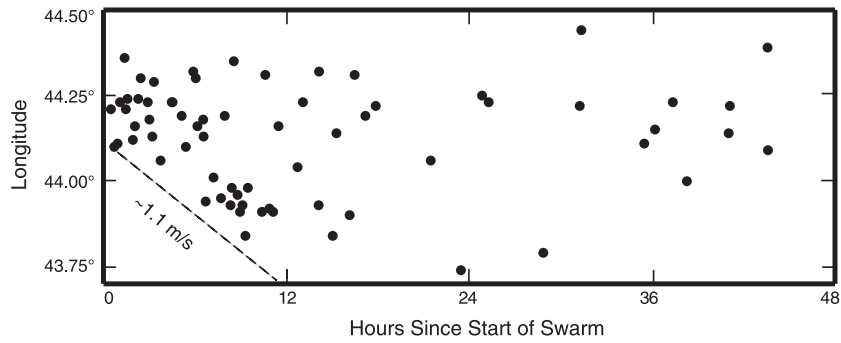


**Figure 5.** Spatial and temporal distribution of earthquakes for the first 48 hr of the swarm. Earthquakes are plotted as black circles at the longitude of their centroid locations. The time plotted in this figure is relative to the start of the swarm, November 14 at 06:32 GMT. For reference, a propagation rate of  $1.1 \text{ m s}^{-1}$  is indicated by the dashed line. This is a maximum estimate for the propagation rate of the onset of seismicity.

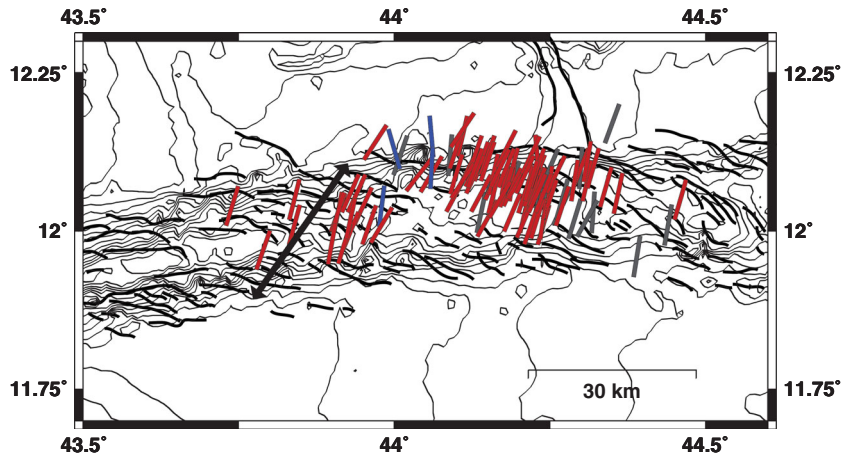


**Figure 6.** Azimuths of tension axes for the western Gulf of Aden earthquakes. Tension axes are plotted at the centroid locations, and are drawn in blue for earthquakes with large strike-slip components, and red or grey for the best constrained and less well-constrained normal-faulting earthquakes. The double-headed black arrow shows the spreading direction from the global plate motion model MORVEL (DeMets *et al.* 2010). Black lines show fault traces from Dauteuil *et al.* (2001). Bathymetry from GEBCO is plotted in 100-m contours. Tension axes are plotted in chronological order, and a single, early strike-slip event at  $12.09^\circ\text{N}$ ,  $44.2^\circ\text{E}$  is obscured by later normal-faulting events.

is given to events with the smallest number of usable data, typically the result of small magnitude and/or the presence of large amplitude waveforms from other earthquakes. Nonetheless, focal mechanisms for the least well-constrained earthquakes are consistent with those of the best-constrained events (Figs 4 and 6), and we do not distinguish between them in the discussion below.

Although we report complete deviatoric moment tensors for the western Gulf of Aden earthquakes in Table S1, we plot only the double-couple components of the focal mechanisms in Fig. 4 because we are unable to constrain the non-double-couple component well using the existing data. There are few close stations, and many of the earthquakes are near the magnitude threshold of GCMT analysis. The largest normal-faulting earthquakes have small non-double-couple components, and are consistent with rupture on planar faults. Larger non-double-couple components are retrieved for the least well-constrained earthquakes and earthquakes with strike-slip focal mechanisms, but for these events we find that double-couple moment tensors fit the data nearly as well as the full solutions. The strikes and dips of the nodal planes for the two types of solutions are nearly identical.

The standard errors for the latitude and longitude components of the centroid locations are between 3 and 5 km on average (Table S1). Owing to uneven station distributions, the presence of noise and unmodelled structural heterogeneity (Nakanishi &

Kanamori 1982; Smith & Ekström 1997; Hjörleifsdóttir & Ekström 2010), we believe that the actual errors are likely to be larger. The good correspondence between the centroid locations and the axial valley, however, suggest that absolute location errors are typically less than 20 km. Because the distances between individual earthquakes in the sequence are small, and because we use a similar station distribution for each CMT solution, the relative location errors are expected to be smaller, approximately 5–10 km.

The western Gulf of Aden swarm is dominated by normal-faulting earthquakes located in the axial valley between  $43.75^\circ$  and  $44.5^\circ\text{E}$  (Fig. 4). These earthquakes have WNW–ESE striking nodal planes that are oriented  $\text{N}109^\circ\text{E}$  on average, or  $\sim 75^\circ$  from the direction of relative plate motion (DeMets *et al.* 2010). The rotation of the nodal planes with respect to the spreading-orthogonal direction is consistent with fault populations at other oblique rifts around the world (Taylor *et al.* 1994; Tuckwell *et al.* 1996). The normal-faulting earthquakes have dip angles that are close to  $45^\circ$ , with the average dip angles of the shallow and steep nodal planes being  $42^\circ$  and  $51^\circ$ , respectively. For these events, there is excellent agreement between the distribution of retrieved strike angles of the nodal planes and observed fault orientations measured using acoustic reflectivity data (Dauteuil *et al.* 2001). Though the vast majority of the earthquakes show normal faulting, a small fraction of the earthquakes have strike-slip focal mechanisms with NE–SW

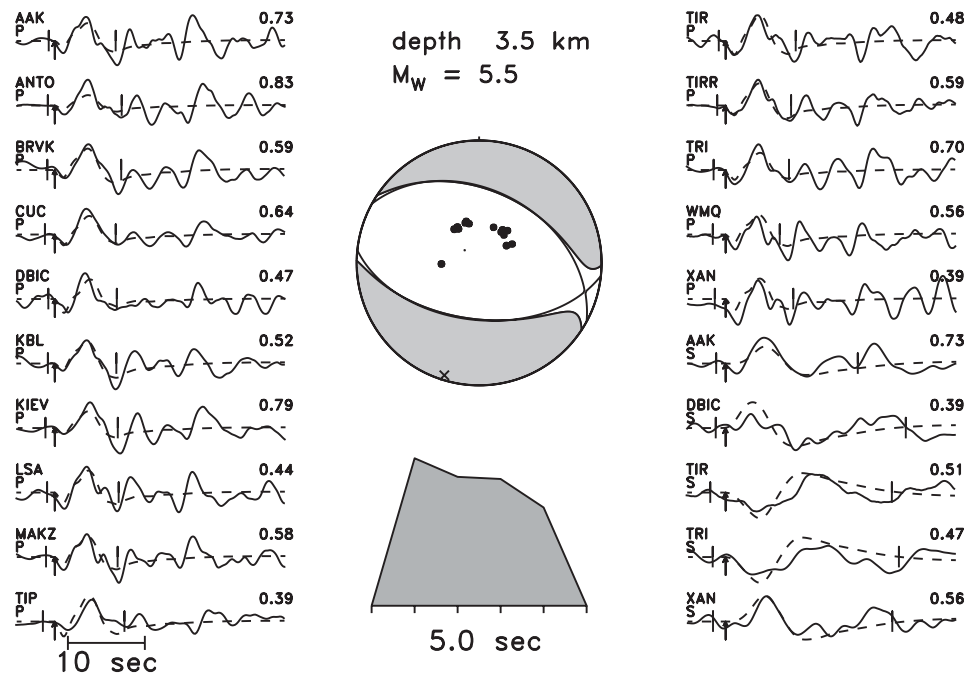


**Figure 7.** Focal-depth analysis for the  $M_w$  5.5 earthquake on 2010 November 14 at 17:02 GMT. Solid lines are broad-band teleseismic  $P$  and  $SH$  waveforms, and dashed lines are synthetic seismograms. Brackets across the waveforms show the portions of the seismograms that were used in the inversion, and arrows indicate the picked first arrivals. The station names and maximum amplitude (in microns) are printed for each waveform. The focal mechanism and moment-rate function determined by the body-wave inversion are plotted in the centre of the figure. Solid black lines on the focal mechanism show nodal planes for the double-couple part of the moment tensor. Black dots on the focal mechanism show where the plotted waveforms exited the focal sphere. The focal depth of the earthquake is 3.5 km below the sea surface, or 2.3 km below the seafloor.

**Table 1.** Focal-depth estimates determined by broad-band analysis. The depths are relative to the seafloor.

Earthquake date and time	$M_w$	Depth (km)
11/14/10 06:32	5.4	1.6
11/14/10 13:50	5.2	2.6
11/14/10 17:02	5.5	2.3
11/14/10 22:22	5.3	1.8

and NW–SE striking nodal planes, consistent with the extension direction.

The western Gulf of Aden earthquakes are clustered in both space and time. Spatially, the centroid locations are divided into two elongated groups, which are offset from one another by 10–15 km (Fig. 4). These groups correspond to mapped basins inside the axial valley, east and west of  $44^\circ\text{E}$  (Dauteuil *et al.* 2001). Although normal-faulting earthquakes are distributed throughout the basins, strike-slip earthquakes are predominantly located near the offset between two of the basins near  $44^\circ\text{E}$ . At the beginning of the sequence, the basins east of  $44^\circ\text{E}$  were active, producing four of the 10 largest earthquakes observed during the entire sequence within the first 6 hr. Beginning at 12:49 on November 14, activity shifted to the western basin for approximately 10 hr and produced the remaining six of the 10 largest earthquakes. From November 15 onwards, seismicity continued at a lower rate and was concentrated east of  $44^\circ\text{E}$ . We do not find any evidence for uniform migration of the centroids with time. However, we do observe a westward propagation of the onset of seismicity for the first 12 hr of the swarm, as shown in Fig. 5. We find that seismicity migrated at a rate no higher than  $\sim 1.1 \text{ m s}^{-1}$ , which is consistent with earthquake swarms from Iceland and Afar (Brandsdóttir & Einarsson 1979; Belachew *et al.* 2011).

The principal axes of the moment tensor provide information about the strain accommodated by fault movements (McKenzie 1969; Townend 2006). The tension axes indicate the direction of maximum extension during an earthquake. Tension axes are close to horizontal for both normal-faulting and strike-slip earthquakes in the western Gulf of Aden sequence, and the azimuths of the tension axes we determine are plotted in Fig. 6. For normal-faulting earthquakes, the average azimuth of the tension axes is  $\text{N}19^\circ\text{E}$ , which is intermediate between the spreading direction from global plate motion vectors,  $\text{N}34^\circ\text{E}$  (DeMets *et al.* 2010), and the normal to the ridge trend in this area,  $\text{N}20^\circ\text{W}$ – $\text{N}0^\circ\text{E}$ . These observations are consistent with earthquake focal mechanisms at other oblique rifts around the world (Fournier & Petit 2007), as well as with the orientations of normal-fault structures observed in analogue models of oblique rifting (Withjack & Jamison 1986; Tron & Brun 1991; Clifton *et al.* 2000). The tension axes of the strike-slip earthquakes near  $44^\circ\text{E}$  are rotated counter-clockwise relative to those of the normal-faulting earthquakes, as expected for a left-stepping transform fault connecting two ridge segments. The full deviatoric moment tensors for these earthquakes are also consistent with composite focal mechanisms resulting from earthquakes with subevents on both ridge and transform segments with this left-stepping geometry (Frohlich 1994). The strike-slip earthquakes likely indicate that the offset between basins near  $44^\circ\text{E}$  is a transfer zone (Dauteuil & Brun 1993; Bellahsen *et al.* 2006; Autin *et al.* 2010), in the process of developing into a transform fault, as has already occurred east of the Shukra al Sheik discontinuity.

## 5.2 Teleseismic body wave modelling

We are able to model the teleseismic body waves of four earthquakes, all occurring on 2010 November 14. The first of these

earthquakes occurred east of 44°E, whereas the remaining earthquakes are located in the western basin. Although the focal depth estimates depend on the particular choice of crustal model, we find that, for reasonable choices of sediment thickness ranging from 0–1 km, the waveforms can be fit well and the differences between focal depth estimates are well within the 1–2 km uncertainty associated with the Ekström (1989) method. An example of the waveform fits achieved is shown in Fig. 7. In Table 1, we present focal depths that were calculated using a velocity model that includes a 1.25-km layer of water and a 1-km layer of sediments. This model was chosen to account for the fact that the sediment thickness in the western Gulf of Aden ranges from essentially zero near the ridge axis to 2 km outside the rift (Khanbari 2000 as cited in Hébert *et al.* 2001). The focal depths we retrieve are shallow, ranging from 1.6 to 2.6 km below the seafloor. If we use a sediment thickness of 0 km, the focal depth estimates range from 1.4 to 2.4 km below the seafloor. These depth estimates are consistent with other earthquakes from mid-ocean ridges with similar spreading rates (Huang & Solomon 1988). For  $M_w$  5.5 normal-faulting earthquakes, empirical scaling relationships estimate the downdip fault width to be ~5 km (Wells & Coppersmith 1994), so it is likely that some of the earthquakes in this sequence ruptured the surface of the seafloor. If indeed 1 km of sediments is present, our depth estimates suggest that the earthquakes occurred only ~0.5–1.5 km into the crystalline crust. Such shallow depth estimates suggest either the earthquakes had unusually high stress drops, unlikely if the earthquakes occurred on pre-existing faults, or that seismogenic rupture continued into the sediment layer.

## 6 DISCUSSION

The western Gulf of Aden earthquake sequence occurred beneath more than a kilometre of water in one of the most dangerous shipping routes in the world (Smith *et al.* 2011). Thus, there are no independent observations of the deformation that took place during this episode, either from satellite interferometry or from ship-based surveys. However, the character of the seismic activity is similar to dyke-induced earthquake sequences observed in both continental and oceanic settings, and we infer that this sequence is the seismic component of a magmatic rifting episode. We base this interpretation on the swarm-like nature of the sequence, and the dominance of normal-faulting earthquakes clustered around the ridge axis. With this interpretation, we estimate the duration of the dyking event and the amount of opening that took place along this section of the ridge. We use published analogue models to interpret our observations in the context of the evolution of the Gulf of Aden and other oblique rifts around the world.

### 6.1 Comparison to other dyke-induced rifting episodes

During rifting episodes along mid-ocean ridges and magma-rich segments of continental rifts, both dykes and faults accommodate plate boundary separation. As dykes propagate laterally through the crust, they trigger slip on faults located above and ahead of the intrusions (Rubin & Pollard 1988; Rubin 1992; Rubin & Gillard 1998). After propagation ceases, earthquakes continue to occur on pre-existing faults close to failure because of changes in Coulomb stress caused by the dyke injection and related faulting and thermal stressing, although these earthquakes are generally fewer in number (Toda *et al.* 2002; Ayele *et al.* 2009; Kulpinski *et al.* 2009; Ebinger *et al.* 2010). Dyke-induced rifting episodes in both continental and

oceanic settings are characterized by earthquake sequences that have neither a single large main shock nor a decrease in magnitude with time (Abdallah *et al.* 1979; Brandsdóttir & Einarsson 1979; Tolstoy *et al.* 2001; Wright *et al.* 2006; Rowland *et al.* 2007; Ebinger *et al.* 2008, 2010; Ayele *et al.* 2009; Keir *et al.* 2009; Riedel & Schlindwein 2010). Such swarms have elevated  $b$  values, which are typically attributed to high thermal gradients and the presence or migration of magmatic and/or hydrothermal fluids (Brandsdóttir & Einarsson 1979; King 1983; Hill *et al.* 1990; Wiemer & McNutt 1997; Wiemer *et al.* 1998; Toda *et al.* 2002; Farrell *et al.* 2009).

For the western Gulf of Aden sequence, we estimated the  $b$ -value by examining the frequency-magnitude distribution. The magnitude of completeness ( $M_c$ ) was defined as the magnitude below which the data depart from a linear trend by more than one standard deviation (Zúñiga & Wyss 1995). Using the maximum likelihood approach (Aki 1965; Utsu 1965; Bender 1983; Wiemer 2001) with a  $M_c$  of  $M_w$  4.8 and calculating the uncertainty by bootstrapping, we estimate the  $b$ -value for the western Gulf of Aden sequence to be  $1.6 \pm 0.18$ , which is significantly higher than the global average value of ~1.0 (Frohlich & Davis 1993). The estimate of  $b$ -value remains well above 1.0 for choices of  $M_c$  larger than 4.8.

Although there is some debate over whether particular earthquake swarms on mid-ocean ridges result from episodes of tectonic extension or magmatism (Bergman & Solomon 1990), dyke-induced earthquake swarms have now been observed directly on many mid-ocean ridges. Along fast and intermediate-spreading mid-ocean ridges, dyke intrusions produce short-lived swarms of  $M_w \leq 4.0$  earthquakes that are observed primarily by ocean-bottom seismometers (Dziak *et al.* 1995, 2007, 2009; Fox *et al.* 1995; Tolstoy *et al.* 2006), whereas larger, teleseismically detected swarms of dyke-induced earthquakes are generally only located on slow and ultra-slow spreading ridges such as the Mid-Atlantic Ridge and the Gakkal Ridge (Müller & Jokat 2000; Tolstoy *et al.* 2001; Dziak *et al.* 2004; Riedel & Schlindwein 2010; Schlindwein & Riedel 2010; Korger & Schlindwein 2011). For normal-faulting earthquakes along mid-ocean ridges, an inverse relationship between maximum earthquake size and spreading rate has been observed, and is attributed to thermal limitations on the depth of the seismogenic zone (Solomon & Burr 1979; Huang & Solomon 1988; Bird *et al.* 2009).

The mid-ocean ridge swarm that is most similar to the swarm investigated in this study is the 1999 Gakkal Ridge swarm, which lasted 9 months and produced 20 normal-faulting earthquakes with  $M_w \geq 5.0$  (Müller & Jokat 2000; Tolstoy *et al.* 2001; Ekström *et al.* 2003; Riedel & Schlindwein 2010). In that case, sonar images and bathymetric data suggest that the swarm was associated with a volcanic eruption on the seafloor (Edwards *et al.* 2001). As at the Gakkal Ridge, the large magnitudes of the earthquakes in this study can likely be attributed in part to the slow spreading rate in the western Gulf of Aden.

The regional crustal structure and tectonic history of the western Gulf of Aden may also help explain the large magnitudes of the earthquakes. The area of the earthquake swarm has thick crust, which is transitional from oceanic to continental (Dauteuil *et al.* 2001; Hébert *et al.* 2001), and thicker sections of brittle crust can support larger earthquakes (Rubin 1990). Large earthquakes have also been associated with dykes that are the first to intrude host rift zones after long periods of quiescence (Rubin & Gillard 1998). Based on the seismic history and on the seafloor observations of Dauteuil *et al.* (2001), this rifting episode is the first in the western Gulf of Aden in a minimum of several decades, and may represent westward propagation of active seafloor spreading into a new section of the Aden Ridge.



This interpretation of rift propagation is consistent with the fact that the earthquake swarm that most closely resembles the western Gulf of Aden sequence, continental or oceanic, occurred on an incipient mid-ocean ridge in neighbouring Afar. The 2005 September dyking episode in Afar was characterized by hundreds of teleseismically detected, shallow earthquakes located in a 120-km-long by 25-km-wide area of the Dabbahu segment of the Red Sea rift over a period of 3 weeks. These earthquakes were predominantly normal faulting and 17 had  $M_w \geq 5.0$  (Ebinger *et al.* 2008, 2010; Ayele *et al.* 2009). Like the western Gulf of Aden sequence, the largest magnitude earthquake in the 2005 Afar rifting episode was  $M_w$  5.5 and the cumulative seismic moment was equivalent to a single  $M_w$  6.3 earthquake (Ebinger *et al.* 2008; Grandin *et al.* 2009). InSAR studies confirm that a magma volume of 1.5–2.5 km<sup>3</sup> was injected along a 65-km-long shallow dyke during the 2005 Afar rifting episode (Wright *et al.* 2006; Grandin *et al.* 2009).

Because the western Gulf of Aden sequence has elevated  $b$ -value and is dominated by shallow, normal-faulting earthquakes that migrate over time, closely resembling well-documented dyke-induced earthquake sequences in both oceanic and continental settings, we conclude that this swarm represents the seismic component of a magmatic rifting episode along the nascent Aden Ridge. The large size of the earthquakes likely results from the combined effects of the slow spreading rate, relatively thick crust and recent quiescence.

## 6.2 Rifting episode duration and opening estimates

The similarities between the earthquakes in this study and those associated with the well-documented Afar rifting episodes enable us to make a rough estimate of the duration of the dyke intrusion, as well as the amount of opening that took place during the 2010 rifting episode. Belachew *et al.* (2011) performed a detailed analysis of local seismic data from nine dyke intrusions in Afar, and concluded that the largest earthquakes in each sequence were caused by faulting and graben formation above laterally propagating dyke intrusions. Based on cumulative seismic moment curves, they conclude that the vast majority of seismic moment is accumulated during the dyke propagation phase, after which seismicity decreases significantly, and the slope of the cumulative seismic moment curve flattens. Interpreting our cumulative seismic moment curve (Fig. 3) in the same way, we estimate that the main dyke intrusion in the western Gulf of Aden propagated for less than 18 hr. This result is consistent with our observation that seismicity migrated westwards for approximately 12 hr during the beginning of the swarm. Combining these results, we conclude that the dyke propagation phase during the 2010 western Gulf of Aden rifting episode likely lasted between 12 and 18 hr. This is shorter than the dyke propagation phase for the 2005 rifting episode in Afar, which lasted several days (Ayele *et al.* 2009).

Using our CMT solutions, and assuming that all extension occurs on planar normal faults, we estimate the amount of spreading accommodated by the earthquakes using the following expression:

$$\sum M_0 = \mu L h d / (\sin(\theta) \cos(\theta)), \quad (1)$$

modified from Solomon *et al.* (1988). Here,  $\sum M_0$  is the cumulative seismic moment of the normal-faulting earthquakes,  $\mu$  is the shear modulus,  $h$  is the thickness of the seismogenic layer,  $\theta$  is the dip of the fault planes,  $L$  is the total along-axis length of the ridge segments that slipped in the earthquakes and  $d$  is the total amount of horizontal opening. We use values of  $3.0 \times 10^{10}$  N m<sup>-2</sup> for  $\mu$ , and 10 km for  $h$  (Dauteuil *et al.* 2001), and calculate the remaining

parameters from the CMT solutions.  $\sum M_0$  is  $3.4 \times 10^{18}$  Nm, and we estimate  $L$  from the distance between the easternmost and westernmost earthquake centroids, finding a value of 80 km. We use  $51^\circ$  for  $\theta$ , which is the average dip angle for the steeply dipping nodal planes. Because all of the retrieved nodal-plane dips are close to this value, the result depends little on the details of this choice. Solving for the horizontal displacement, we obtain a value of  $d \approx 7$  cm, which is equivalent to  $\sim 4$  yr of spreading assuming that opening occurs solely by seismogenic extension of the brittle lithosphere at a rate of 1.63 cm yr<sup>-1</sup>, the full spreading rate predicted by MORVEL for  $12^\circ$ N,  $44^\circ$ E (DeMets *et al.* 2010). If instead we constrain  $h$  to be 5 km, the downdip width for the largest earthquakes based on our depth and scalar moment estimates and scaling relationships of Wells & Coppersmith (1994), the estimate of horizontal opening is twice as large,  $d \approx 14$  cm, which is equivalent to  $\sim 8$  yr of spreading.

However, the amount of opening that occurred during the western Gulf of Aden rifting episode is likely to be much higher. Along slow-spreading mid-ocean ridges, earthquakes account for no more than 10–20 per cent of plate separation (Solomon *et al.* 1988). Rifting episodes in continental settings are also generally dominated by aseismic deformation. In Iceland, the Asal Rift and Afar, field measurements of fault offsets from rifting episodes are much larger than the amount of slip required to generate the observed earthquake swarms (Brandsdóttir & Einarsson 1979; Doubré & Peltzer 2007; Rowland *et al.* 2007). Additional aseismic opening may occur because of the volume change associated with the dyke intrusion. The discrepancy between seismogenic and total opening can also be demonstrated by comparing the cumulative seismic moment to estimates of the combined geodetic moment, which accounts for dip slip on normal faults and volume change because of magma intrusions. For the 2005 September rifting episode in Afar, the geodetic moment was at least an order of magnitude larger than the cumulative seismic moment (Wright *et al.* 2006; Grandin *et al.* 2009). Belachew *et al.* (2011) compared the seismic and geodetic moments for nine rifting episodes in Afar between 2006 and 2009, and found that earthquakes accounted for only  $\sim 0.1$ – $3.5$  per cent of the total deformation. Following Solomon *et al.* (1988) and Belachew *et al.* (2011), if we assume that 1–5 per cent of the total deformation was accommodated by earthquakes, we estimate that this discrete rifting episode may have accommodated  $\sim 1$ – $14$  m of opening, or  $\sim 85$ – $800$  yr of spreading, in this section of the western Gulf of Aden.

## 6.3 Evolution of the western Gulf of Aden

The Gulf of Aden is a transtensional setting where rift formation results from oblique divergence. The relative amounts of extension and shear, and therefore the faulting patterns that are produced along a given section of the rift, depend on the obliquity angle,  $\alpha$ , which is the angle between the rift trend (N70–90°E) and the direction of relative plate motion (N34°E; DeMets *et al.* 2010). The obliquity angle in the western Gulf of Aden varies between  $\sim 35^\circ$  and  $55^\circ$  in the area of the recent earthquake swarm, with the highest value of  $\alpha$  being found east of  $44^\circ$ E where the rift trends east-west. For similar values of  $\alpha$ , analogue models show that oblique rifting produces en echelon arrays of normal faults in the axial valley (Withjack & Jamison 1986; Tron & Brun 1991; Dauteuil & Brun 1993; McClay & White 1995; Clifton *et al.* 2000; Mart & Dauteuil 2000; Clifton & Schlische 2001; Corti *et al.* 2001, 2003; Agostini *et al.* 2009; Autin *et al.* 2010). In the models,



these normal faults strike in a direction intermediate between rift parallel and perpendicular to the spreading direction (Withjack & Jamison 1986; Clifton *et al.* 2000; Corti *et al.* 2001, 2003; Autin *et al.* 2010). The orientations of the nodal planes from our CMT solutions support these results. For normal-faulting earthquakes, the average strike angle of the nodal planes is N109°E, which is intermediate between N70–90°E and N124°E. Analytical models demonstrate that these fault patterns arise because the combination of extension and shear in oblique rifts results in the principal extensional strain being oriented approximately halfway between the normal to the rift trend and the spreading direction (Withjack & Jamison 1986). The strain pattern we find in the western Gulf of Aden provides observational validation of this explanation. The mean orientation of the tension axes we observe in the swarm is N19°E, intermediate between north–south and the direction of relative plate motion, N34°E.

Overall, there is excellent agreement between the results of our seismic analysis and models of oblique rifting, which allows us to remark on the both the current and future states of the rift system in the western Gulf of Aden. Recent scaled analogue models by Autin *et al.* (2010) suggest that the oblique rifting in the Gulf of Aden was not initiated on a pre-existing weak zone, so that the structures that develop are not influenced by previous geometry. Their work, as well as other analogue models (Clifton & Schlische 2001; Agostini *et al.* 2009), indicate that the western Gulf of Aden is in the late stages of oblique rifting, where deformation is largely controlled by slip on pre-existing fault segments. The similarity between the orientations of faults mapped before the earthquake swarm (Dauteuil *et al.* 2001) and the nodal planes of the normal-faulting earthquakes supports the interpretation that the 2010 swarm occurred on pre-existing faults in the axial valley. Based on the analogue models, we expect that further extension will result in additional slip and lengthening of optimally oriented echelon normal faults (Clifton *et al.* 2000; Clifton & Schlische 2001; Agostini *et al.* 2009). In addition, we expect that some of the transfer zones between individual basins may evolve towards transform faults (Dauteuil & Brun 1993; Bellahsen *et al.* 2006; Autin *et al.* 2010), and segmentation of the ridge will increase as seafloor spreading develops in the western Gulf of Aden. The occurrence of strike-slip earthquakes in the 2010 swarm, near a step over between basins and a change in ridge orientation at 44°E, may indicate the presence of an incipient transform fault.

In analogue models of oblique rifts, normal faults in the axial valley control the emplacement of magmatic intrusions and define the locations of ocean accretion centres (Clifton & Schlische 2001; Agostini *et al.* 2009; Autin *et al.* 2010). This progression has already been documented within basins east of the recent swarm, where seafloor spreading is more developed and there are linear chains of volcanoes oriented N110°–120°E (Tamsett & Searle 1988; Dauteuil *et al.* 2001). Before 2010, the section of the rift where the swarm is located was characterized by low levels of seismicity and a lack of recent volcanism, and gravity and magnetic surveys indicated that seafloor spreading had not yet been initiated (Dauteuil *et al.* 2001; Hébert *et al.* 2001). We believe that the earthquakes in the 2010 swarm are the seismic component of a dyke-induced rifting episode, which provides evidence for westward propagation of seafloor spreading into this area. As in Afar, this swarm confirms that deformation at the onset of seafloor spreading is achieved by intense episodes of dyke intrusion and faulting. For now it is unknown whether this rifting episode will consist of a single dyking episode, like in the Asal Rift in 1978 (Abdallah *et al.* 1979), or whether additional dyke intrusion episodes will follow as in Afar

and Iceland. If the latter, we expect additional dyke intrusions to become progressively more effusive, leading to eruptions on the seafloor (Buck *et al.* 2006; Hamling *et al.* 2010).

## 7 CONCLUSIONS

In the western Gulf of Aden, the east–west trending boundary between the Arabian and Somalian plates is transitioning from a continental rift to a mid-ocean ridge. Until recently, the section of the nascent Aden Ridge near 44°E was characterized by low levels of seismicity and a lack of recent volcanism on the seafloor, and has been believed to lie west of the boundary of active seafloor spreading. However, our analysis of a swarm of moderate to large earthquakes that began on 2010 November 14 in this area indicates that the early stages of seafloor spreading have now propagated into this section of the rift. The swarm closely resembles dyke-induced earthquake swarms from both continental and oceanic settings, and was likely triggered by the lateral propagation of a shallow dyke intrusion. Though the sequence was dominated by shallow, normal-faulting earthquakes, we also find evidence for an incipient transform fault and the early stages of rift-transform segmentation. The direction of extension accommodated by the normal-faulting earthquakes of the sequence is intermediate between the rift orthogonal and the spreading direction predicted by global plate motion vectors, validating analogue and analytical models of oblique rifting. Our findings indicate that deformation at the onset of seafloor spreading is achieved by discrete episodes of faulting and magmatism.

## ACKNOWLEDGMENTS

We thank G. Ekström, C.J. Ebinger and M. Belachew for helpful comments and discussions. We also thank A. Rubin, Editor Y. Ben-Zion and one anonymous reviewer for constructive comments that improved the manuscript. The seismic data used in this paper were collected and distributed by IRIS and the USGS. We thank the operators of the GSN, Geoscope, GEOFON, MEDNET and the Canadian National Seismic Network for collecting and archiving the seismic data used in this study. This work was supported by NSF award EAR-0944055.

## REFERENCES

- Abdallah, A. *et al.*, 1979. Relevance of Afar seismicity and volcanism to the mechanics of accreting plate boundaries, *Nature*, **282**, 17–23.
- Agostini, A., Corti, G., Zeoli, A. & Mulugeta, G., 2009. Evolution, pattern, and partitioning of deformation during oblique continental rifting: inferences from lithospheric-scale centrifuge models, *Geochem. Geophys. Geosyst.*, **10**, doi:10.1029/2009GC002676.
- Aki, K., 1965. Maximum likelihood estimate of  $b$  in the formula  $\log N = a - bM$  and its confidence limits, *Bull. Earthq. Res. Inst. Univ. Tokyo*, **43**, 237–239.
- Arvidsson, R. & Ekström, G., 1998. Global CMT analysis of moderate earthquakes,  $M_w \geq 4.5$ , using intermediate-period surface waves, *Bull. seism. Soc. Am.*, **88**, 1003–1013.
- Autin, J., Bellahsen, N., Husson, L., Beslier, M.-O., Leroy, S. & d'Acremont, E., 2010. Analog models of oblique rifting in a cold lithosphere, *Tectonics*, **29**, doi:10.1029/2010TC002671.
- Ayele, A. *et al.*, 2009. September 2005 mega-dike emplacement in the Manda-Harraro nascent oceanic rift (Afar depression), *Geophys. Res. Lett.*, **36**, doi:10.1029/2009GL039605.

- Baker, J., Snee, L. & Menzies, M., 1996. A brief Oligocene period of flood volcanism in Yemen: implications for the duration and rate of continental flood volcanism at the Afro-Arabian triple junction, *Earth planet. Sci. Lett.*, **138**, 39–55, doi:10.1016/0012-821X(95)00229-6.
- Bassin, C., Laske, G. & Masters, G., 2000. The current limits of resolution for surface wave tomography in North America, *EOS, Trans. Am. geophys. Un.*, **81**(48), Fall. Meet. Suppl., Abstract T31B-1820.
- Belachew, M., Ebinger, C., Coté, D., Keir, D., Rowland, J.V., Hammond, J.O.S. & Ayele, A., 2011. Comparison of dike intrusions in an incipient seafloor-spreading segment in Afar, Ethiopia: seismicity perspectives, *J. geophys. Res.*, **116**, doi:10.1029/2010JB007908.
- Bellahsen, N., Faccenna, C., Funicello, F., Daniel, J.-M. & Jolivet, L., 2003. Why did Arabia separate from Africa?: insights from 3-D laboratory experiments, *Earth planet. Sci. Lett.*, **216**, 365–381.
- Bellahsen, N., Fournier, M., d'Acremont, E., Leroy, S. & Daniel, J.M., 2006. Fault reactivation and rift localization: northeastern Gulf of Aden margin, *Tectonics*, **25**, doi:10.1029/2004TC001626.
- Bender, B., 1983. Maximum likelihood estimation of b values for magnitude grouped data, *Bull. seism. Soc. Am.*, **73**, 831–851.
- Bergman, E.A. & Solomon, S.C., 1990. Earthquake swarms on the Mid-Atlantic Ridge: products of magmatism or extensional tectonics?, *J. geophys. Res.*, **95**, 4943–4965.
- Bird, P., 2003. An updated digital model of plate boundaries, *Geochem. Geophys. Geosyst.*, **4**, doi:10.1029/2001GC000252.
- Bird, P., Kagan, Y.Y., Jackson, D.D., Schoenberg, F.P. & Werner, M.J., 2009. Linear and nonlinear relations between relative plate velocity and seismicity, *Bull. seism. Soc. Am.*, **99**, 3097–3113, doi:10.1785/0120090082.
- Bosworth, W., Huchon, P. & McClay, K., 2005. The Red Sea and Gulf of Aden Basins, *J. Afr. Earth Sci.*, **43**, 334–378.
- Brandsdóttir, B. & Einarsson, P., 1979. Seismic activity associated with the September 1977 deflation of the Krafla central volcano in northeastern Iceland, *J. Volc. Geotherm. Res.*, **6**, 197–212.
- Buck, W.R., Einarsson, P. & Brandsdóttir, B., 2006. Tectonic stress and magma chamber size as controls on dike propagation: constraints from the 1975–1984 Krafla rifting episode, *J. geophys. Res.*, **111**, doi:10.1029/2005JB003879.
- Clifton, A.E. & Schlische, R.W., 2001. Nucleation, growth, and linkage of faults in oblique rift zones: results from experimental clay models and implications for maximum fault size, *Geology*, **29**, 455–458.
- Clifton, A.E., Schlische, R.W., Withjack, M.O. & Ackermann, R.V., 2000. Influence of rift obliquity on fault-population systematics: results of experimental clay models, *J. Struct. Geol.*, **22**, 1491–1509.
- Cochran, J.R., 1981. The Gulf of Aden: structure and evolution of a young ocean basin and continental margin, *J. geophys. Res.*, **86**, 263–287.
- Corti, G., Bonini, M., Innocenti, F., Manetti, P. & Mulugeta, G., 2001. Centrifuge models simulating magma emplacement during oblique rifting, *J. Geodyn.*, **31**, 557–576.
- Corti, G., Bonini, M., Conticelli, S., Innocenti, F., Manetti, P. & Sokoutis, D., 2003. Analogue modeling of continental extension: a review focused on the relations between the patterns of deformation and the presence of magma, *Earth-Sci. Rev.*, **63**, 169–247.
- Courtillot, V.E., 1980. Opening of the Gulf of Aden and Afar by progressive tearing, *Phys. Earth planet. Inter.*, **21**, 343–350.
- Courtillot, V., Jaupart, C., Manighetti, I., Tapponnier, P. & Besse, J., 1999. On causal links between flood basalts and continental breakup, *Earth planet. Sci. Lett.*, **166**, 177–195.
- Dauteuil, O. & Brun, J.-P., 1993. Oblique rifting in a slow-spreading ridge, *Nature*, **361**, 145–148.
- Dauteuil, O., Huchon, P., Quemeneur, F. & Souriot, T., 2001. Propagation of an oblique spreading center: the western Gulf of Aden, *Tectonophysics*, **332**, 423–442.
- DeMets, C., Gordon, R.G. & Argus, D.F., 2010. Geologically current plate motions, *Geophys. J. Int.*, **181**, doi:10.1111/j.1365-246X.2009.04491.x.
- Doubré, C. & Peltzer, G., 2007. Fluid-controlled faulting process in the Asal rift, Djibouti, from 8 yr of radar interferometry observations, *Geology*, **35**, doi:10.1130/G23022A.1.
- Dziak, R.P., Fox, C.G. & Schreiner, A.E., 1995. The June–July 1993 seismo-acoustic event at CoAxial segment, Juan de Fuca Ridge: evidence for a lateral dike injection, *Geophys. Res. Lett.*, **22**, doi:10.1029/94GL01857.
- Dziak, R., Smith, D., Bohnenstiehl, D., Fox, C., Desbruyeres, D., Matsumoto, H., Tolstoy, M. & Fornari, D., 2004. Evidence of a recent magma dike intrusion at the slow-spreading Lucky Strike segment, Mid-Atlantic Ridge, *J. geophys. Res.*, **109**, doi:10.1029/2004JB003141.
- Dziak, R.P., Bohnenstiehl, D.R., Cowen, J.P., Baker, E.T., Rubin, K.H., Haxel, J.H. & Fowler, M.J., 2007. Rapid dike emplacement leads to eruptions and hydrothermal plume release during seafloor spreading events, *Geology*, **35**, doi:10.1130/G23476A.1.
- Dziak, R.P., Bohnenstiehl, D.R., Matsumoto, H., Fowler, M.J., Haxel, J.H., Tolstoy, M. & Waldhauser, F., 2009. January 2006 seafloor-spreading event at 9°50'N, East Pacific Rise: ridge dike intrusion and transform fault interactions from regional hydroacoustic data, *Geochem. Geophys. Geosyst.*, **10**, doi:10.1029/2009GC002388.
- Dziewonski, A.M. & Anderson, 1981. Preliminary Reference Earth Model, *Phys. Earth planet. Inter.*, **25**, 297–356.
- Dziewonski, A.M., Chou, T.-A. & Woodhouse, J.H., 1981. Determination of earthquake source parameters from waveform data for studies of global and regional seismicity, *J. geophys. Res.*, **86**, 2825–2852.
- Ebinger, C.J. *et al.*, 2008. Capturing magma intrusion and faulting processes during continental rupture: seismicity of the Dabbahu (Afar) rift, *Geophys. J. Int.*, **174**, doi:10.1111/j.1365-246X.2008.03877.x.
- Ebinger, C., Ayele, A., Keir, D., Rowland, J., Yirgu, G., Wright, T., Belachew, M. & Hamling, I., 2010. Length and timescales of rift faulting and magma intrusion: the Afar rifting cycle from 2005 to present, *Ann. Rev. Earth planet. Sci.*, **38**, doi:10.1146/annurev-earth-040809-152333.
- Edwards, M.H., Kurras, G.J., Tolstoy, M., Bohnenstiehl, D.R., Coackley, B.J. & Cochran, J.R., 2001. Evidence of recent volcanic activity on the ultraslow-spreading Gakkel Ridge, *Nature*, **409**, 808–812.
- Ekström, G., 1989. A very broad band inversion method for the recovery of earthquake source parameters, *Tectonophysics*, **166**, 73–100.
- Ekström, G., 2006. Global detection and location of seismic sources by using surface waves, *Bull. seism. Soc. Am.*, **96**, doi:10.1785/0120050175.
- Ekström, G., Dziewonski, A.M., Maternovskaya, N.N. & Nettles, M., 2003. Global seismicity of 2001: centroid-moment tensor solutions for 961 earthquakes, *Phys. Earth planet. Inter.*, **136**, 165–185.
- Ekström, G., Dziewonski, A.M., Maternovskaya, N.N. & Nettles, M., 2005. Global seismicity of 2003: centroid-moment-tensor solutions for 1087 earthquakes, *Phys. Earth planet. Inter.*, **148**, 327–351.
- Farrell, J., Husen, S. & Smith, R.B., 2009. Earthquake swarm and b-value characterization of the Yellowstone volcano-tectonic system, *J. Volc. Geotherm. Res.*, **188**, 260–276.
- Fournier, M. & Petit, C., 2007. Oblique rifting at oceanic ridges: relationship between spreading and stretching directions from earthquake focal mechanisms, *J. Struct. Geol.*, **29**, 201–208.
- Fox, C., Radford, W.E., Dziak, R., Lau, T.-K., Matsumoto, H. & Schreiner, A.E., 1995. Acoustic detection of a seafloor spreading episode on the Juan de Fuca ridge using military hydrophone arrays, *Geophys. Res. Lett.*, **22**, doi:10.1029/94GL02059.
- Frohlich, C., 1994. Earthquakes with non-double-couple mechanisms, *Science*, **264**, 804–807.
- Frohlich, C. & Davis, S.D., 1993. Teleseismic b values; or, much ado about 1.0, *J. geophys. Res.*, **98**, 631–644.
- Grandin, R. *et al.*, 2009. September 2005 Manda Hararo-Dabbahu rifting event, Afar (Ethiopia): constraints provided by geodetic data, *J. geophys. Res.*, **114**, doi:10.1029/2008JB005843.
- Hamling, I.J., Wright, T.J., Calais, E., Bennati, L. & Lewi, E., 2010. Stress transfer between thirteen successive dyke intrusions in Ethiopia, *Nature Geosci.*, **3**, doi:10.1038/NGEO967.
- Hébert, H., Deplus, C., Huchon, P., Khanbari, K. & Audin, L., 2001. Lithospheric structure of a nascent spreading ridge inferred from gravity data: the western Gulf of Aden, *J. geophys. Res.*, **106**, 26 345–26 363.
- Hill, D.P. *et al.*, 1990. The 1989 earthquake swarm beneath Mammoth Mountain, California: an initial look at the 4 May through 30 September activity, *Bull. seism. Soc. Am.*, **80**, 325–339.

- Hjörleifsdóttir, V. & Ekström, G., 2010. Effects of three-dimensional Earth structure on CMT earthquake parameters, *Phys. Earth planet. Inter.*, **179**, 178–190, doi:10.1016/j.pepi.2009.11.003.
- Hoffman, C., Courtillot, V., Féraud, G., Rochette, P., Yirgu, G., Ketefo, E. & Pik, R., 1997. Timing of the Ethiopian flood basalt event and implications for plume birth and global change, *Nature*, **389**, 838–841, doi:10.1038/39853.
- Huang, P.Y. & Solomon, S.C., 1988. Centroid depth of Mid-Ocean Ridge earthquakes: dependence on spreading rate, *J. geophys. Res.*, **93**, 13 445–13 477.
- Jolivet, L. & Faccenna, C., 2000. Mediterranean extension and the Africa-Eurasia collision, *Tectonics*, **19**, 1095–1106, doi:10.1029/2000TC900018.
- Keir, D. *et al.*, 2009. Evidence for focused magma accretion at segment centers from lateral dike injections captured beneath the Red Sea rift in Afar, *Geology*, **37**, doi:10.1130/G25147A.1.
- Khanbari, K., 2000. Propagation d'un rift océanique: le Golfe d'Aden, *PhD thesis*, Univ. Paris Sud, Paris, France.
- King, G., 1983. The accommodation of large strains in the upper lithosphere of the earth and other solids by self-similar fault systems: the geometrical origin of b-value, *Pure appl. Geophys.*, **121**, 761–815.
- Korger, E.I.M. & Schlindwein, V., 2011. Performance of localization algorithms for teleseismic mid-ocean ridge earthquakes: the 1999 Gakkel Ridge earthquake swarm and its geological interpretation, *Geophys. J. Int.*, **188**, 613–625, doi:10.1111/j.1365-246X.2011.05282.x.
- Kulpinski, K., Coté, D.M., Ebinger, C.J., Keir, D. & Ayele, A., 2009. Testing models of dike intrusion during rifting episodes: the role of heating in triggering earthquakes in Afar, *EOS, Trans. Am. geophys. Un.*, **9**(52), [Fall Meet. Suppl., Abstract T31B-1820].
- Malkin, B.V. & Shemenda, A.I., 1991. Mechanism of rifting: considerations based on results of physical modeling and on geological and geophysical data, *Tectonophysics*, **199**, 193–210, doi:10.1016/0040-1951(91)90170-O.
- Manighetti, I., Tapponnier, P., Courtillot, V., Gruszow, S. & Gillot, P.-Y., 1997. Propagation of rifting along the Arabia-Somalia plate boundary: the Gulfs of Aden and Tadjoura, *J. geophys. Res.*, **102**, 2681–2710.
- Mart, Y. & Dauteuil, O., 2000. Analogue experiments of propagation of oblique rifts, *Tectonophysics*, **316**, 121–132.
- McClay, K.R. & White, M.J., 1995. Analogue modeling of orthogonal and oblique rifting, *Mar. Pet. Geol.*, **12**, 137–151.
- McKenzie, D.P., 1969. The relation between fault plane solutions for earthquakes and the directions of the principal stress, *Bull. seism. Soc. Am.*, **59**, 591–601.
- Müller, C. & Jokat, W., 2000. Seismic evidence for volcanic activity discovered in Central Arctic, *EOS, Trans. Am. geophys. Un.*, **81**, 265–269.
- Nakanishi, I. & Kanamori, H., 1982. Effects of lateral heterogeneity and source process time on the linear moment tensor inversion of long-period Rayleigh-waves, *Bull. seismol. Soc. Am.*, **72**, 2063–2080.
- Riedel, C. & Schlindwein, V., 2010. Did the 1999 earthquake swarm on Gakkel Ridge open a volcanic conduit? A detailed teleseismic data analysis, *J. Seismol.*, **14**, 505–522.
- Rochette, P. *et al.*, 1997. Magnetostratigraphy and timing of the Oligocene Ethiopian traps, *Earth planet. Sci. Lett.*, **14**, 497–510.
- Rowland, J.V., Baker, E., Ebinger, C.J., Keir, D., Kidane, T., Biggs, J., Hayward, N. & Wright, T.J., 2007. Fault growth at a nascent slow-spreading ridge: 2005 Dabbahu rifting episode, Afar, *Geophys. J. Int.*, **171**, 1226–1246.
- Rubin, A.M., 1990. A comparison of rift-zone tectonics in Iceland and Hawaii, *Bull. Volcanol.*, **52**, 302–319.
- Rubin, A.M., 1992. Dike-induced faulting and graben subsidence in volcanic rift zones, *J. geophys. Res.*, **97**, 1839–1858.
- Rubin, A.M. & Pollard, D.D., 1988. Dike-induced faulting in rift zones of Iceland and Afar, *Geology*, **16**, 413–417.
- Rubin, A.M. & Gillard, D., 1998. Dike-induced earthquakes: theoretical considerations, *J. geophys. Res.*, **103**, 10 017–10 030.
- Schlindwein, V. & Riedel, C., 2010. Location and source mechanism of sound signals at Gakkel ridge, Arctic Ocean: submarine Strombolian activity in the 1999–2001 volcanic episode, *Geochem. Geophys. Geosyst.*, **11**, doi:10.1029/2009GC002706.
- Shcherbakov, R. & Turcotte, D., 2004. A modified form of Bath's Law, *Bull. seism. Soc. Am.*, **94**(5), 1968–1975.
- Shcherbakov, R., Turcotte, D. & Rundle, J., 2005. Aftershock statistics, *Pure appl. Geophys.*, **162**, 1051–1076, doi:10.1007/s00024-004-2661-8.
- Smith, G. & Ekström, G., 1997. Interpretation of earthquake epicenter and CMT centroid locations, in terms of rupture length and direction, *Phys. Earth planet. Inter.*, **102**, 123–132.
- Smith, S.R., Bourassa, M.A. & Long, M., 2011. Pirate attacks affect Indian Ocean climate research, *EOS, Trans. Am. geophys. Un.*, **92**, 225–226.
- Solomon, S.C. & Burr, N.C., 1979. The relationship of source parameters of ridge-crest and transform earthquakes to the thermal structure of oceanic lithosphere, *Tectonophysics*, **55**, 107–126.
- Solomon, S.C., Huang, P.Y. & Meinke, L., 1988. The seismic moment budget of slowly spreading ridges, *Nature*, **334**, 58–60.
- Tamsett, D. & Searle, R.C., 1988. Structure and development of the Mid-ocean Ridge plate boundary in the Gulf of Aden: evidence from GLORIA side scan sonar, *J. geophys. Res.*, **93**, 3157–3178.
- Taylor, B., Crook, K. & Sinton, J., 1994. Extensional transform zones and oblique spreading centers, *J. geophys. Res.*, **99**, 19 707–19 718.
- Toda, S., Stein, R.S. & Sagiya, T., 2002. Evidence from the AD 2000 Izu islands earthquake swarm that stressing rate governs seismicity, *Nature*, **419**, 58–61.
- Tolstoy, M., Bohnenstiehl, D.R., Edwards, M.H. & Kurras, G.J., 2001. Seismic character of volcanic activity at the ultraslow-spreading Gakkel Ridge, *Geology*, **29**, 1139–1142.
- Tolstoy, M. *et al.*, 2006. A sea-floor spreading event captured by seismometers, *Science*, **314**, 1920–1922.
- Townend, J., 2006. What do faults feel? observational constraints on the stresses acting on seismogenic faults, in *Earthquakes: Radiated Energy and the Physics of Faulting*, Geophys. Monogr. Ser. Vol. 170, pp. 313–327, eds Abercrombie, R., McGarr, A., Di Toro, G. & Kanamori, H., American Geophysical Union, Washington, DC.
- Tron, V. & Brun, J.-P., 1991. Experiments on oblique rifting in brittle-ductile systems, *Tectonophysics*, **188**, 71–84.
- Tuckwell, G.W., Bull, J.M. & Sanderson, D.J., 1996. Models of fracture orientation at oblique spreading centers, *J. geol. Soc. Lond.*, **153**, 185–189.
- Ukstins, I.A., Renne, P.R., Wolfenden, E., Baker, J., Ayalew, D. & Menzies, M., 2002. Matching conjugate volcanic rifted margins: 40Ar/39Ar chronostratigraphy of the pre- and syn-rift bimodal flood volcanism in Ethiopia and Yemen, *Earth planet. Sci. Lett.*, **198**, 289–306, doi:10.1016/S0012-821X(02)00525-3.
- Utsu, T., 1965. A method for determining the value of *b* in a formula  $\log N = a - bM$  showing the magnitude frequency for earthquakes, *Geophys. Bull. Hokkaido Univ.*, **13**, 99–103.
- Wells, D.L. & Coppersmith, K.J., 1994. New Empirical relationships among magnitude, rupture length, rupture width, rupture area, and surface displacement, *Bull. seism. Soc. Am.*, **84**, 974–1002.
- Wiemer, S., 2001. A software package to analyze seismicity: ZMAP, *Seismol. Res. Lett.*, **72**, 374–383.
- Wiemer, S. & McNutt, S.R., 1997. Variations in the frequency-magnitude distribution with depth in two volcanic areas: Mount St. Helens, Washington, and Mt. Spurr, Alaska, *Geophys. Res. Lett.*, **24**, 189–192.
- Wiemer, S., McNutt, S.R. & Wyss, M., 1998. Temporal and three-dimensional spatial analyses of the frequency-magnitude distribution near Long Valley Caldera, California, *Geophys. J. Int.*, **134**, 409–421.
- Withjack, M.O. & Jamison, W.R., 1986. Deformation produced by oblique rifting, *Tectonophysics*, **126**, 99–124.
- Wright, T.J., Ebinger, C., Biggs, J., Ayele, A., Yirgu, G., Keir, D. & Stork, A., 2006. Magma-maintained rift segmentation at continental rupture in the 2005 Afar dyking episode, *Nature*, **442**, doi:10.1038/nature04978.



Zúñiga, R. & Wyss, M., 1995. Inadvertent changes in magnitude reported in earthquake catalogs: their evaluation through *b*-value estimates, *Bull. seism. Soc. Am.*, **85**, 1858–1866.

## SUPPORTING INFORMATION

Additional Supporting Information may be found in the online version of this article:

**Table S1.** Centroid-moment-tensor solutions for 110 earthquakes occurring in the Western Gulf of Aden, 11/2010–4/2011.

**Table S2.** Principal axes and best-double-couple parameters.

Please note: Wiley-Blackwell are not responsible for the content or functionality of any supporting materials supplied by the authors. Any queries (other than missing material) should be directed to the corresponding author for the article.